*Progress In Electromagnetics Research M, Vol. 79, 11–22, 2019*

# Design and Analysis of $\mu$-Negative Material Loaded Wideband Electrically Compact Antenna for WLAN/WiMAX Applications

**Upesh Patel* and Trushit Upadhyaya**

**Abstract**—A compact tri-band antenna incorporated with a split ring resonator array is proposed for Wireless Local Area Network (WLAN) and Worldwide interoperability for microwave access (WiMAX) applications. The proposed antenna is printed on an FR4 substrate with overall dimensions of $0.25\lambda \times 0.29\lambda$ at the lowest frequency. Impedance bandwidth of the antenna is optimised by introducing slots on the top of the patch. The ground plane is engineered by placement of a split ring resonators array to induce additional resonance due to occurance of magnetic dipole moment. The antenna resonates at the frequencies of 2.4 GHz, 3.5 GHz & 5.5 GHz having bandwidths of 12.5%, 7.42% and 6.36% with the gains of 2.25 dBi, 3.72 dBi and 2.71 dBi, respectively which matches well with the fabricated results. The proposed antenna shows omnidirectional radiation pattern which makes it appropriate for WLAN and WiMAX applications.

## 1. INTRODUCTION

With ever increasing demand of wireless communication devices, the need for low profile and multi-band antennas is significantly rising. Multiband planar antennas have significant importance in wireless communication systems. From the RF engineer perspective such antennas should have compact size, high efficiency, and easy fabrication. The antennas should also have application specific sufficient bandwidth and gain. Patch antennas typically suffer from issue of narrow bandwidth. There are many bandwidth and gain enhancement techniques proposed in the literature such as introduction of differently shaped slots [1], multilayer antennas [1, 2], using electromagnetic bandgap materials [3] to name a few. This paper presents utilization of negative refractive index material in conjunction with an engineered ground plane to create multiband and wideband resonance of the patch antenna.

Split-ring resonator, a $\mu$-negative block of negative refractive index material, generates strong magnetic dipole moment under the exposure of time varying field. The frequency dependent permeability can be given as [4]

$$\mu_r(\omega) = 1 - \frac{F\omega^2}{\omega^2 - \omega_0^2 - j\omega\gamma_m} \tag{1}$$

where $\omega_0$ is the resonance frequency, $F$ the unit-cell filling factor, and $\gamma_m$ the damping coefficient. As per Lortenz model, the split ring resonator shall produce negative permeability while $\omega_0 < \omega < \omega_{pm}$. The $\omega_{pm}$ is the magnetic resonance frequency.

Effective use of left handed materials, also known as metamaterials, can increase antenna radiation properties [5, 6]. The dimensions of basic building block of metamaterial should have sub-wavelength in order of $\lambda/10$ or lesser for optimal effect of negative refraction. Negative refractive

*Received 15 December 2018, Accepted 22 January 2019, Scheduled 12 February 2019*

* Corresponding author: Upesh Patel (upeshpatel.ec@charusat.ac.in).
The authors are with the Electronics & Communication Engineering Department, Charotar University of Science & Technology, India.

index materials have provided many benefits to antenna community. It has shown significant aid in antenna miniaturization [7, 8], improvement in cross polarization levels [9], and improvement in radiation efficiency through impedance matching [10]. Recent research in negative refractive index inspired antennas has presented attractive finding in terms of electrically compact antennas [11, 12], MIMO antennas [13, 14], satellite and far field communication antennas [15, 16], beam-tilted antennas [17, 18], reconfigurable antennas [19–21], wideband antennas [22, 23], body centric antennas [24], and energy harvesting antenna [25].

## 2. ANTENNA DESIGN

The proposed antenna geometry along with design parameters is illustrated in Figure 1(a). The proposed structure got evolved from a traditional patch antenna design with the objectives of achieving electrical compactness and reasonable antenna bandwidth and gain. The symmetrical slotted rectangular antenna having area of $32 \times 37.2\,\text{mm}^2$ was matched at $50\,\Omega$. A cost effective FR-4 substrate of 1.6 mm having relative permittivity of 4.4 and loss tangent of 0.008 was utilized for the design. Split ring resonators along with partial ground plane strips are utilized at the antenna bottom face, as illustrated in Figures 1(c) and 1(d), to improve the antenna radiation characteristics. The engineered antenna parameters are tabulated in Table 1.

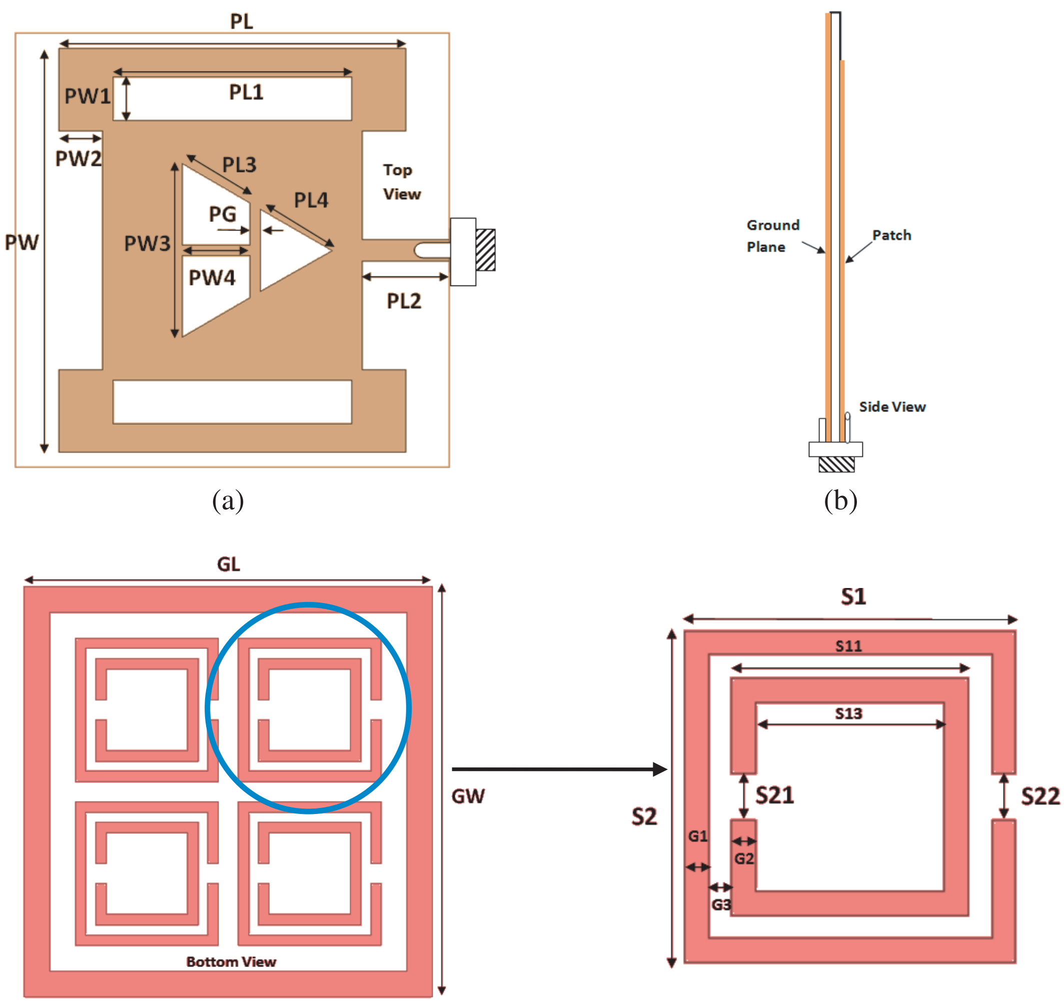


(a) (b) (c) (d)

**Figure 1.** Proposed antenna geometry. (a) Top view, (b) side view, (c) bottom view, (d) unit cell.

**Table 1.** Antenna physical dimensions. All dimensions are in mm.

| **PL** | **PW** | **PL1** | **PL2** | **PL3** | **PL4** | **PW1 = PW2** | **PW4** |
|---|---|---|---|---|---|---|---|
| 32 | 37.2 | 22 | 8 | 7.1 | 7.6 | 4 | 6.2 |
| **S21 = S22** | **GL = GW** | **PG = G1** | **S1 = S2** | **PW3** | **S11** | **S13** | **G2 = G3** |
| 2 | 40 | 1 | 14 | 15.9 | 10 | 8 | 1 |

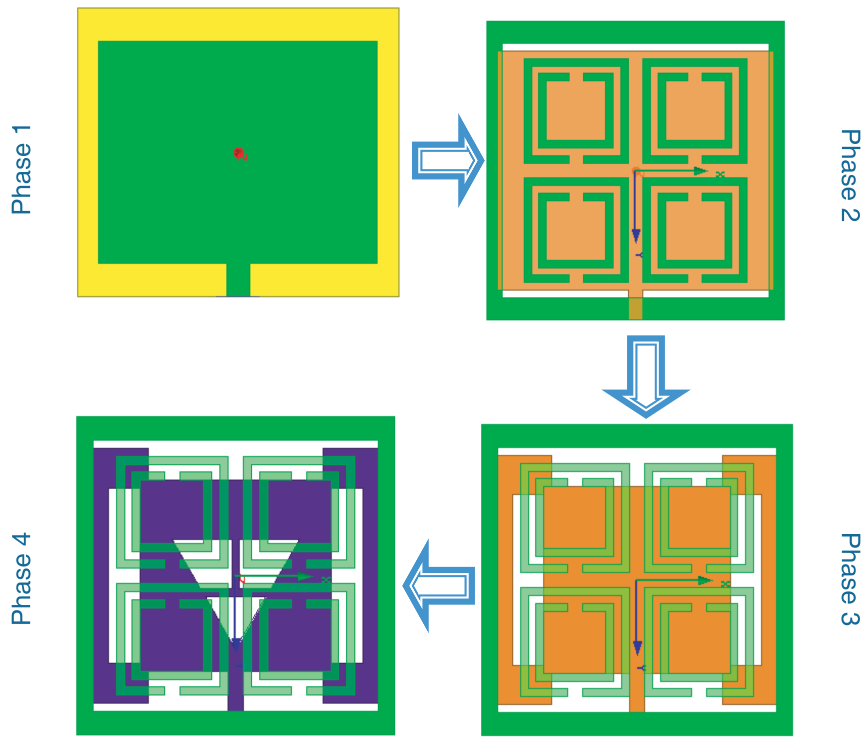


**Figure 2.** Antenna phasewise evolution.

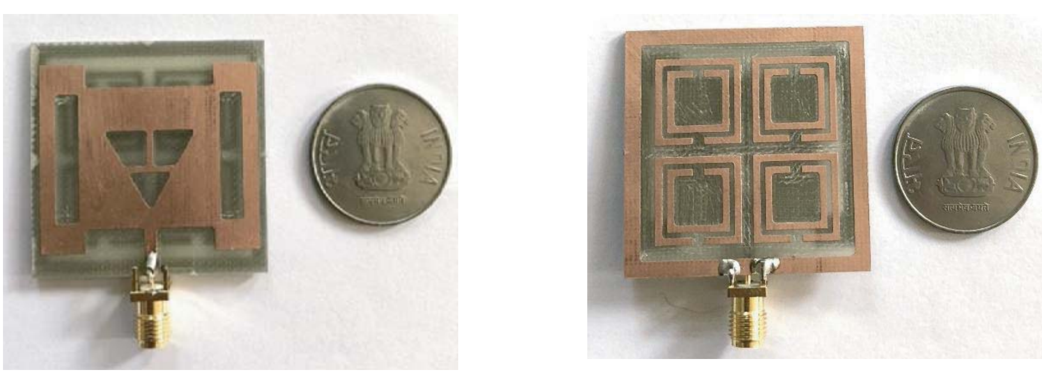

(a) (b)

**Figure 3.** Fabricated prototype of proposed antenna. (a) Top view, (b) bottom view.

The design evolved in four phases. During the first phase of antenna design, two resonant modes were achieved and were further tuned by introducing partial ground plane. The ground plane consisted of rectangular conducting strips adjacent to all sides of the patch. In the second phase, equally spaced

$2 \times 2$ SRR arrays in $x$-$y$ plane at the antenna ground plane were further inducted to achieve additional resonant modes. In the third phase of the design, equidistance symmetric slots at the sides of the patch were created to improve the antenna bandwidth which was further improved by creating center slots in Phase 4. All four design phases are illustrated in Figure 2. The image of fabricated prototype is shown in Figure 3.

## 3. SIMULATED AND MEASURED RESULTS

The phase-wise simulated reflection coefficients of the antenna are shown in Figure 4. The simulation of antenna is carried out using FEM based High-Frequency Structure Simulator (HFSS). The antenna has three resonant modes at center frequencies of 2.4 GHz, 3.5 GHz, and 5.5 GHz. This satisfies the requirement of WLAN and WiMAX frequency bands. The simulated Voltage Standing Wave Ratios (VSWRs) at 2.4 GHz, 3.5 GHz, and 5.5 GHz are 1.09, 1.02, and 1.36, respectively, which meet the primary design criteria of the proposed antenna of having VSWR lesser than 1.5. Owing to high $Q$-factor of the proposed antenna, bandwidth is restricted at higher two bands. After carrying out multiple simulation iterations in Phase-4 of the design, higher bandwidth was achieved. The bandwidth is in order of 12.5% (2220 MHz–2520 MHz), 7.42% (3420 MHz–3680 MHz), and 6.36% (5300 MHz–5650 MHz), respectively for aforementioned frequency bands.

The simulated and measured resonances are illustrated in Figure 5. Return loss and VSWR are measured using key sight VNA 9912A. The SMA connector is connected to the radiator through standard soldering technique. Minor mismatch in these results is due to fabrication inaccuracies and environmental variations between simulation and actual measurements. The simulated current

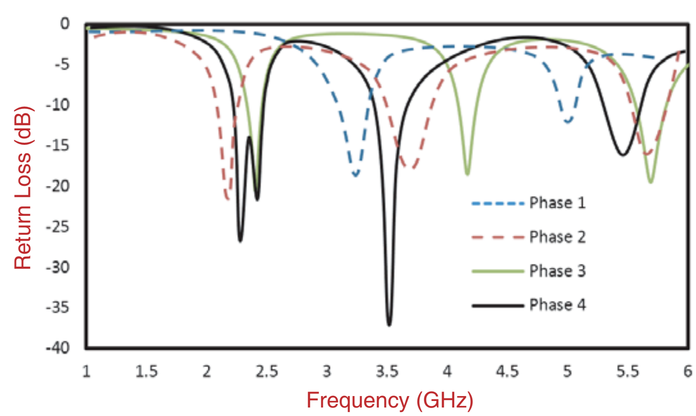


**Figure 4.** Phase wise antenna resonance.

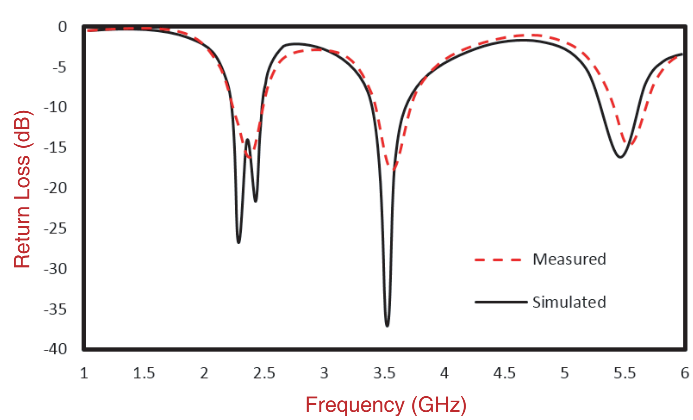


**Figure 5.** Simulated and measured return loss.

distributions of antenna at three resonances are illustrated in Figure 6. The current is not only present near the feed line, but also largely distributed on the antenna near the edges. The current density concentration increases near the slot edges at higher frequencies.

### 3.1. Current Distribution

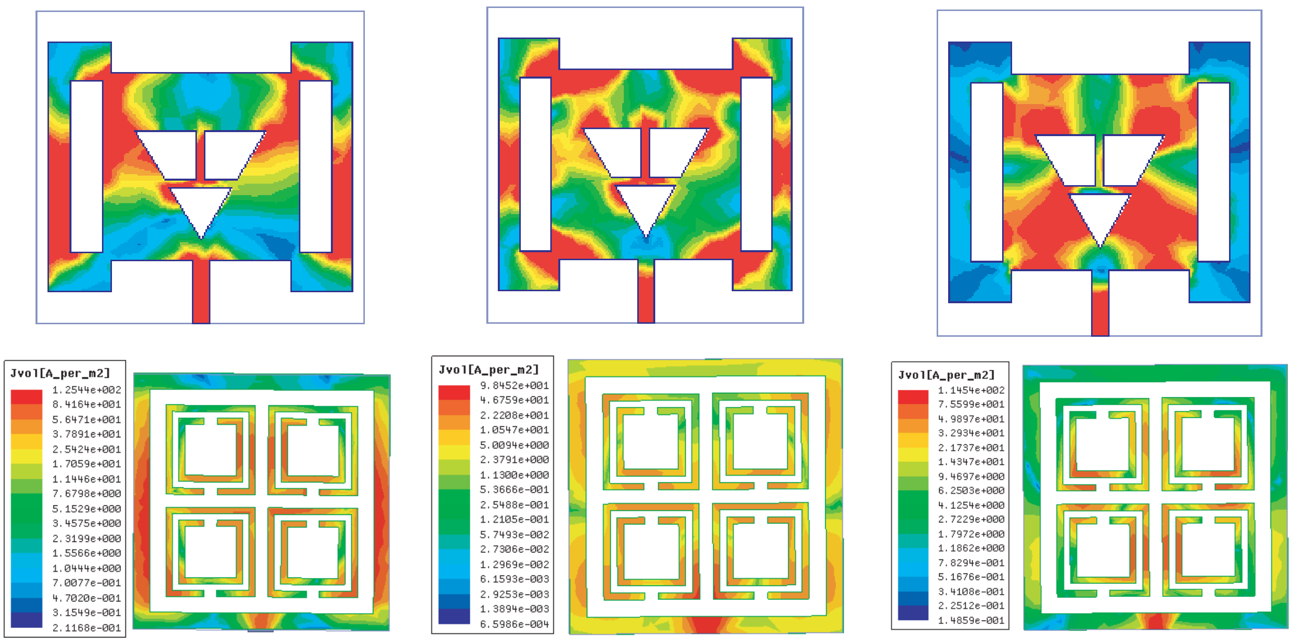


(a) (b) (c)

**Figure 6.** Current distribution at excited modes. (a) 2.4 GHz, (b) 3.5 GHz, (c) 5.5 GHz.

### 3.2. Parametric Study

An open ended design by use of multiple slots on the radiator provides ample opportunity for antenna tuning and performance optimization. The optimal dimensions of the proposed antenna were selected after carrying out rigorous parametric analysis. An increase in antenna width and length causes reduction in resonance as apparent from Figures 7(a) and 7(b). The decrease in PW1, slot along with width, causes decrement in fundamental mode resonance; however, the second and third resonances are increased as visible in Figure 7(c). The increase in PL1, the slot dimensions along the length appearing

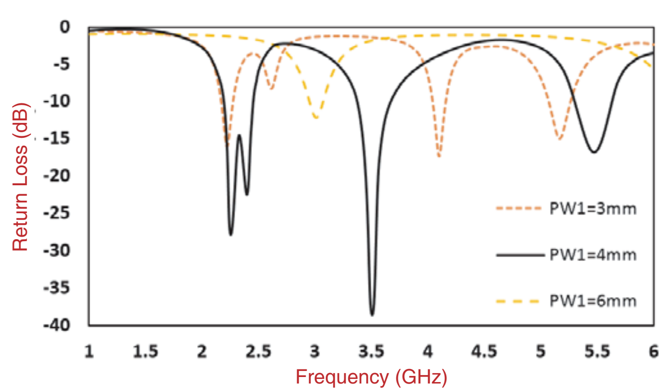


(a)

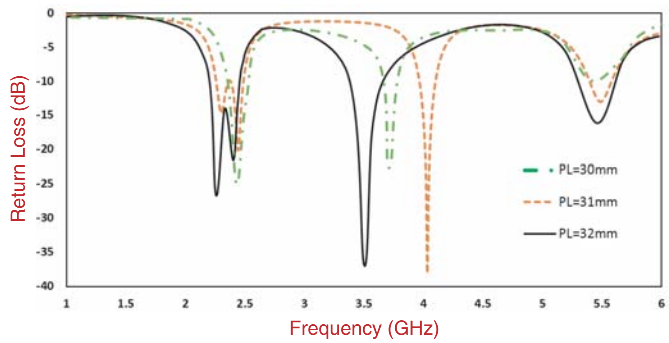


(b)

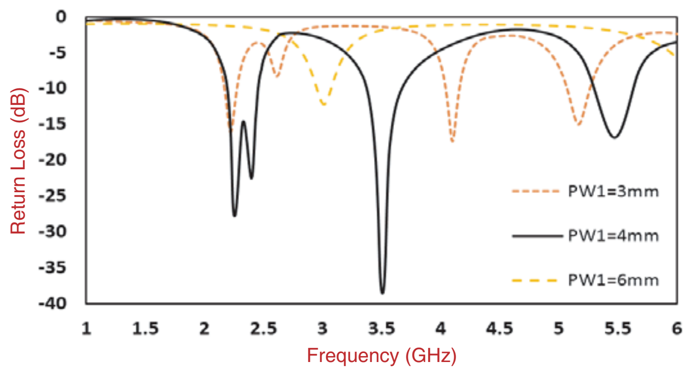


(c)

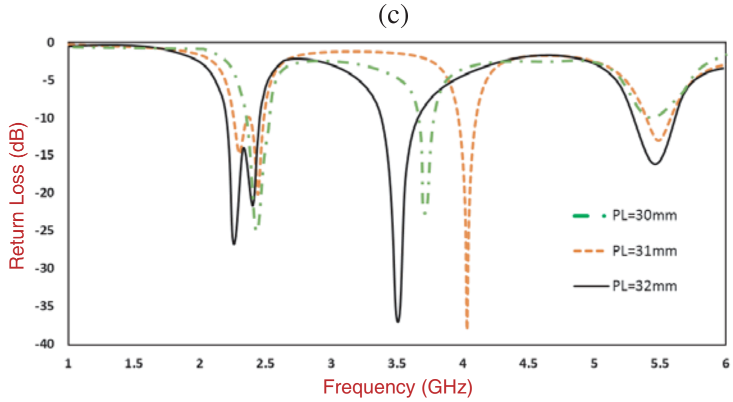


(d)

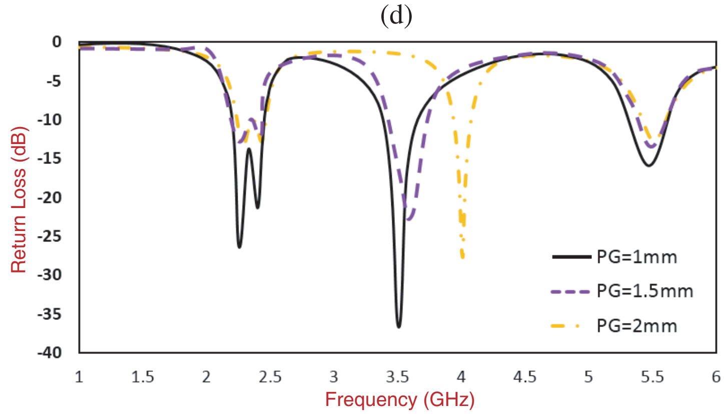


(e)

**Figure 7.** Noticeable physical variations of antenna. (a) Variation in antenna width, (b) variation in patch length, (c) variation in slot dimension along the antenna width, (d) variation in slot dimensions along the antenna length, (e) variations in central triangular slit along the antenna length.

in Figure 7(d), yields decrease in antenna resonance for both fundamental and higher order resonant modes. The variations in central slit increase the return loss for all frequencies, and optimal dimensions are selected for target applications which are illustrated in Figure 7(e).

### 3.3. Radiation Pattern

Antenna radiation pattern measurement in far field ($R \gg \frac{2D^2}{\lambda}$) was carried out in an anechoic chamber as depicted in Figure 8. The $E$-field and $H$-field radiation patterns of the proposed antenna at 2.4 GHz, 3.5 GHz, and 5.5 GHz are shown in Figure 9. The antenna exhibits directive patterns. The directivity can be further improved by employing reflectors. The $H$-plane radiation pattern is quasi-omnidirectional, which suits the design requirement. Use of a standard gain horn antenna along with MATLAB based software simulator was carried out to measure the antenna gain. The gain transfer procedure was used for calculating the antenna gain. The antenna gain can be given as [2]:

$$G_T = G_R = \frac{1}{2}\left[20\log_{10}\left(\frac{4\pi R}{\lambda}\right) + 10\log_{10}\left(\frac{P_R}{P_T}\right)\right] \tag{2}$$

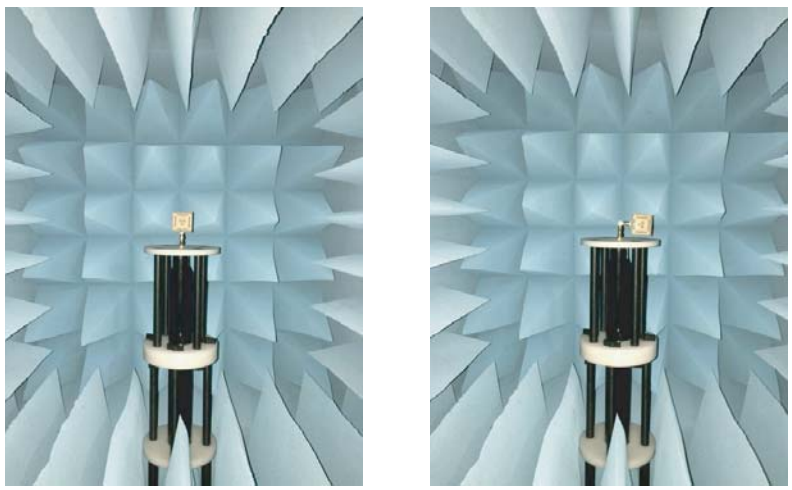

(a) (b)

**Figure 8.** Antenna measurement in anechoic chamber. (a) $E$-plane measurement, (b) $H$-plane measurement.

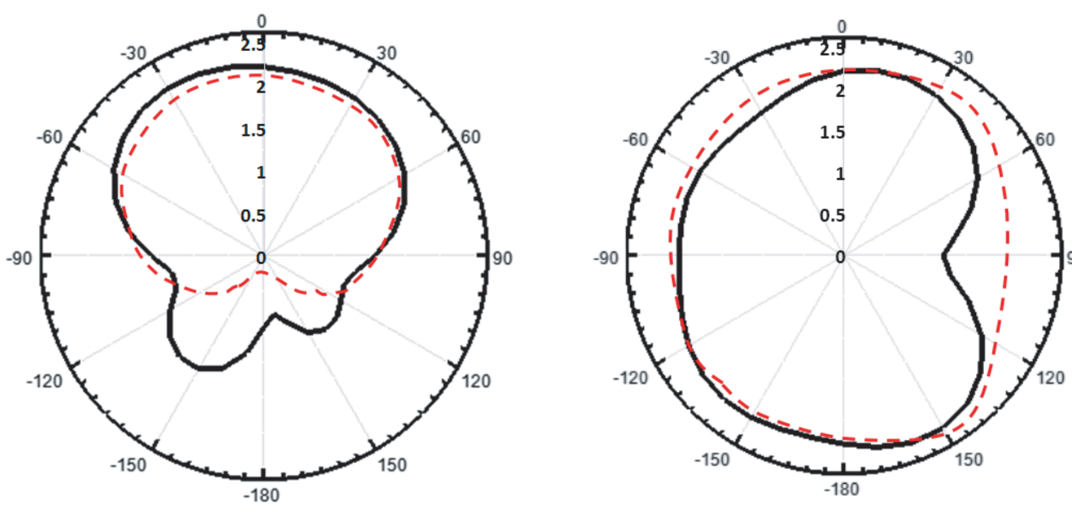


(a) (b)

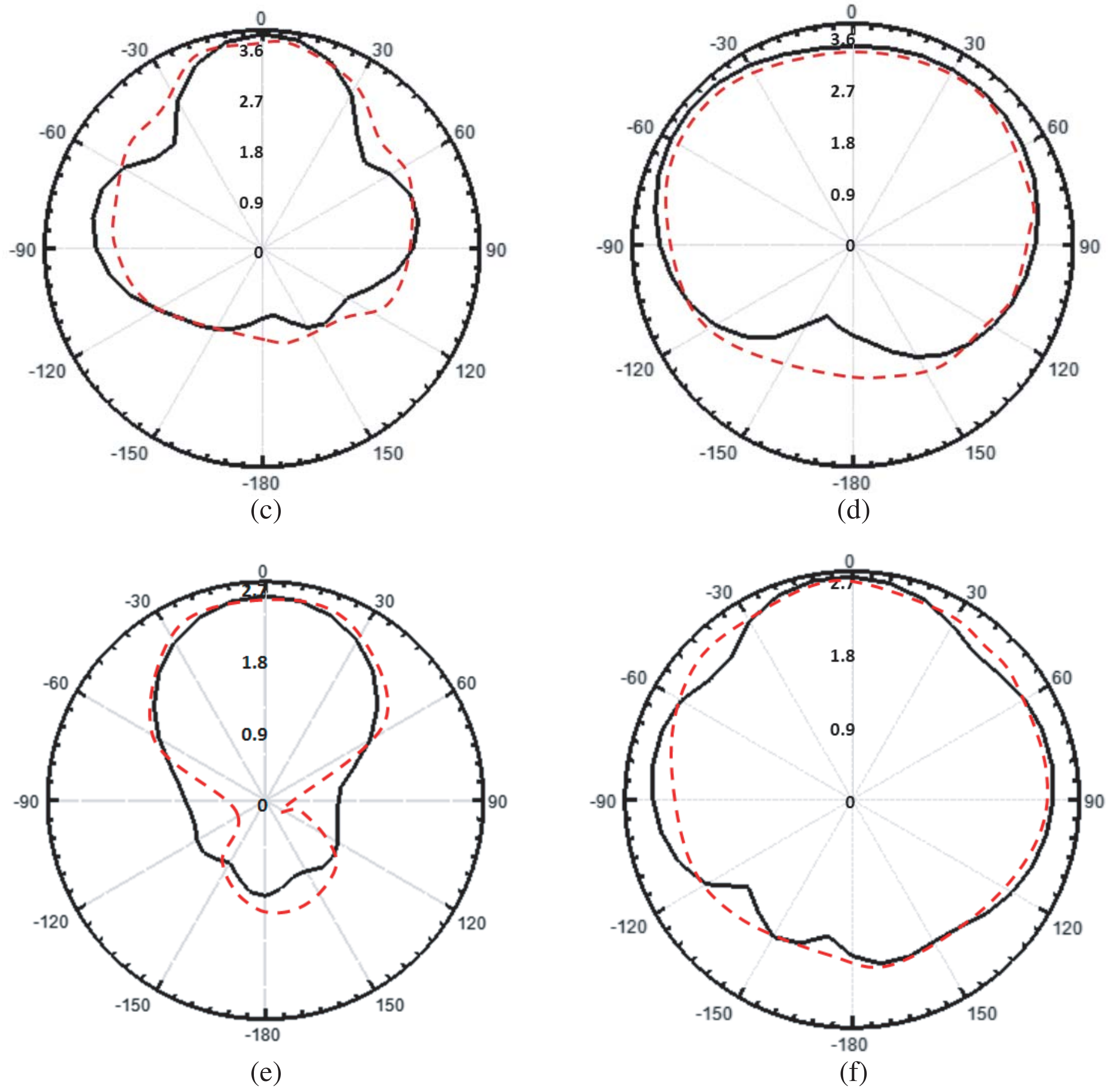


**Figure 9.** Antenna radiation pattern (simulated (solid line), measured (dashed line)). (a) 2.4 GHz $E$-plane, (b) 2.4 GHz $H$-plane, (c) 3.5 GHz $E$-plane, (d) 3.5 GHz $H$-plane, (e) 5.5 GHz $E$-plane, (f) 5.5 GHz $H$-plane.

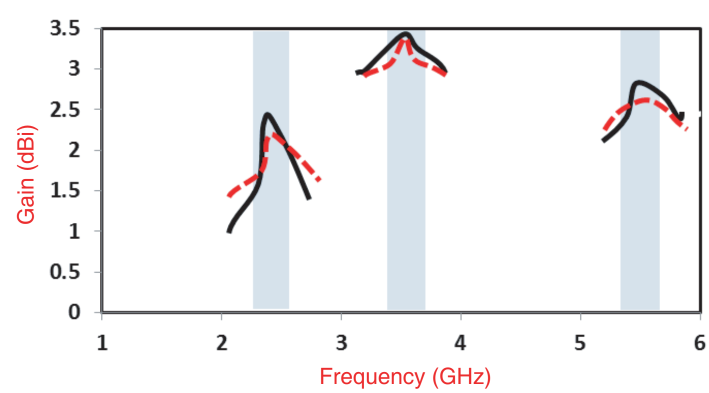


**Figure 10.** Simulated (solid) and measured (dashed) antenna gain.

where $G_T$: Transmitting antenna gain (dB); $G_R$: Receiving antenna gain (dB); $P_T$: Transmitted Power (Watts), $P_R$: Receiver power (Watts), and $R$: Distance between transmitting and receiving antenna. Figure 10 illustrates antenna gain against frequency graph. The gain values at 2.4 GHz, 3.5 GHz, and 5.5 GHz are 2.25 dBi, 3.72 dBi, and 2.71 dBi, respectively. The antenna can be further engineered using gain enhancement techniques present in the literature.

The antenna was embedded on a Router board as shown in Figure 11 to analyze the possible degradation in return loss. Figure 12 illustrates that the return loss of mounted antenna is quite lower than actual test of free standing mode. This is primarily due to the modification in effective relative permittivity of the substrate and hence subsequent impedance matching when being mounted on the PCB Board. Further sources of degradation are dielectric casing of router, packaging loss, and extended coaxial cable loss. The mounted antenna however performs at around 2 : 1 VSWR levels after multiple iterations of mounting and adequate placement. This meets the design criteria.

(a) (b)

**Figure 11.** Antenna mounted on router board for return loss measurement. (a) Board bottom view, (b) board front view.

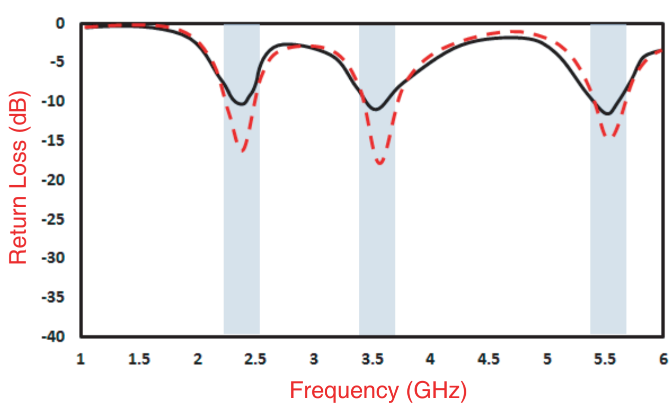


**Figure 12.** Measured return loss when it is free standing (dashed) and when it is installed in router (solid line).

Table 2 provides the performance comparison of the proposed antenna with other relevant designs available in the literature. Antenna parameters such as Physical Size, Gain, and Bandwidth for given dielectric constant of substrate are presented. It is apparent that the proposed antenna has design superiority over many designs in terms of compactness, gain, and bandwidth for the proposed frequency bands.

**Table 2.** Comparison of proposed antenna with related designs in literature.

| Reference | Resonant Center Frequency (GHz) | Gain (dBi) | Bandwidth (%) | Antenna Dimensions ($mm^3$) | Dielectric Constant |
|---|---|---|---|---|---|
| [26] | 2.45, 3.6, 5.5 | 0.76, 0.86, 1.58 | 4.08, 18.88, 20.18 | $20 \times 24 \times 0.635$ | 9.50 |
| [27] | 2.4, 3.5, 5 | 4.5, 4.2, 5.1 | 12.2, 5.6, 7.6 | $75 \times 75 \times 1.6$ | 4.70 |
| [28] | 1.78, 4.22, 5.8 | −1.8, 2.6, 3.1 | 0.8, 15.17, 8.33 | $20 \times 20 \times 0.508$ | 2.33 |
| [29] | 1.57, 1.85, 2.44 | −1, 0, 0.2 | 0.8, 0.5, 0.8 | $41.1 \times 45.5 \times 0.8$ | 3.38 |
| [30] | 2.4, 3.5, 5.8 | 2.0, 1.75, 3 | 13.07, 10.09, 5.09 | $25 \times 22 \times 1.6$ | 4.4 |
| [31] | 2.4, 3.5, 5.5 | 3, 2.25, 4.25 | 12.6, 8, 14.5 | $40 \times 40 \times 0.8$ | 4.4 |
| [32] | 2.5, 3.5, 5.5 | 1, 2.25, 3 | 13.2, 12.57, 15.63 | $35 \times 35 \times 1.6$ | 4.4 |
| [33] | 2.1, 3.45, 5.2 | 1.7, 1.85, 5.38 | 11.2, 5.14, 3.9 | $40 \times 50 \times 1.6$ | 4.4 |
| [34] | 2.4, 3.5, 5.5 | 0.77, 1.98, 1.56 | 6.25, 9.42, 18.72 | $12 \times 23 \times 1$ | 4.65 |
| [35] | 2.61, 3.5, 5.4 | 1.85, 2.19, 2.57 | 11.49, 30, 17.77 | $38 \times 25 \times 1.6$ | 4.4 |
| **Proposed** | **2.4, 3.5, 5.5** | **2.25, 3.72, 2.71** | **12.5, 7.42, 6.36** | $\mathbf{32 \times 37.2 \times 1.6}$ | **4.4** |

## 4. CONCLUSION

A multiband compact metamaterial inspired slotted antenna for WLAN and WiMAX applications was designed and developed. The antenna has compact dimensions of $32 \times 37.2 \times 1.6\,mm^3$. The antenna was embedded into a communication device for analyzing real-time performance. The frequency-dependent permeability of the antenna shall permit further miniaturization by modifying the split ring resonator dimensions; however, predicting antenna resonance due to variations in electromagnetic coupling between split ring resonators is analytically difficult. The parametric study in the proposed designs shows that by merely changing the dimensions on the resonator, it is possible to achieve significant variations in antenna resonance. The design simplicity, return loss, gain, bandwidth, and radiation pattern make the designed antenna a suitable candidate for target applications.

## REFERENCES


1. Kumar, G. and K. P. Ray, *Broadband Microstrip Antennas*, Artech House, 2003.
2. Waterhouse, R., *Microstrip Patch Antennas: A Designer's Guide*, Springer Science & Business Media, 2013.
3. Yang, F. and Y. Rahmat-Samii, *Electromagnetic Band-gap Structures in Antenna Engineering (The Cambridge RF and Microwave Engineering Series)*, Cambridge University Press, 2008.
4. Smith, D. R. and N. Kroll, "Negative refractive index in left-handed materials," *Physical Review Letters*, Vol. 85, No. 14, 2933, 2000.
5. Alibakhshi-Kenari, M., M. Naser-Moghadasi, and R. A. Sadeghzadeh, "Bandwidth and radiation specifications enhancement of monopole antennas loaded with split ring resonators," *IET Microwaves, Antennas & Propagation*, Vol. 9, No. 14, 1487–1496, 2015.
6. Alù, A., F. Bilotti, N. Engheta, and L. Vegni, "Subwavelength, compact, resonant patch antennas loaded with metamaterials," *IEEE Transactions on Antennas and Propagation*, Vol. 55, No. 1, 13–25, 2007.
7. Islam, M. M., M. T. Islam, M. Samsuzzaman, M. R. I. Faruque, N. Misran, and M. F. Mansor, "A miniaturized antenna with negative index metamaterial based on modified SRR and CLS unit cell for UWB microwave imaging applications," *Materials*, Vol. 8, No. 2, 392–407, 2015.
8. Upadhyaya, T. K., V. V. Dwivedi, S. P. Kosta, and Y. P. Kosta, "Miniaturization of tri band patch antenna using metamaterials," *2012 Fourth International Conference on Computational Intelligence and Communication Networks (CICN)*, 45–48, IEEE, November 2012.

9. Upadhyaya, T. K., S. P. Kosta, R. Jyoti, and M. Palandöken, "Novel stacked $\mu$-negative material-loaded antenna for satellite applications," *International Journal of Microwave and Wireless Technologies*, Vol. 8, No. 2, 229–235, 2016.
10. Saraswat, R. K. and M. Kumar, "Miniaturized slotted ground UWB antenna loaded with metamaterial for WLAN and WiMAX applications," *Progress In Electromagnetics Research B*, Vol. 65, 65–80, 2016.
11. Sharma, S. K., M. A. Abdalla, and Z. Hu, "Miniaturisation of an electrically small metamaterial inspired antenna using additional conducting layer," *IET Microwaves, Antennas & Propagation*, Vol. 12, No. 8, 1444–1449, 2018.
12. El Badawe, M., T. S. Almoneef, and O. M. Ramahi, "A true metasurface antenna," *Scientific Reports*, Vol. 6, 19268, 2016.
13. Zhai, G., Z. N. Chen, and X. Qing, "Enhanced isolation of a closely spaced four-element MIMO antenna system using metamaterial mushroom," *IEEE Transactions on Antennas and Propagation*, Vol. 63, No. 8, 3362–3370, 2015.
14. Rezvani, M. and Y. Zehforoosh, "A dual-band multiple-input multiple-output microstrip antenna with metamaterial structure for LTE and WLAN applications," *AEU — International Journal of Electronics and Communications*, Vol. 93, 277–282, 2018.
15. Singh, D. and V. M. Srivastava, "An analysis of RCS for dual-band slotted patch antenna with a thin dielectric using shorted stubs metamaterial absorber," *AEU — International Journal of Electronics and Communications*, Vol. 90, 53–62, 2018.
16. Gupta, N., J. Saxena, K. S. Bhatia, and N. Dadwal, "Design of metamaterial-loaded rectangular patch antenna for satellite communication applications," *Iranian Journal of Science and Technology, Transactions of Electrical Engineering*, 1–11, 2018.
17. Jia, D., Y. He, N. Ding, J. Zhou, B. Du, and W. Zhang, "Beam-steering flat lens antenna based on multilayer gradient index metamaterials," *IEEE Antennas and Wireless Propagation Letters*, Vol. 17, No. 8, 1510–1514, 2018.
18. Upadhyaya, T. K., S. P. Kosta, R. Jyoti, and M. Palandoken, "Negative refractive index material-inspired 90-deg electrically tilted ultra wideband resonator," *Optical Engineering*, Vol. 53, No. 10, 107104, 2014.
19. Rajeshkumar, V. and S. Raghavan, "A compact metamaterial inspired triple band antenna for reconfigurable WLAN/WiMAX applications," *AEU — International Journal of Electronics and Communications*, Vol. 69, No. 1, 274–280, 2015.
20. Cao, W., B. Zhang, A. Liu, T. Yu, D. Guo, and K. Pan, "A reconfigurable microstrip antenna with radiation pattern selectivity and polarization diversity," *IEEE Antennas and Wireless Propagation Letters*, Vol. 11, 453–456, 2012.
21. Johnson, M. C., S. L. Brunton, N. B. Kundtz, and J. N. Kutz, "Sidelobe canceling for reconfigurable holographic metamaterial antenna," *IEEE Transactions on Antennas and Propagation*, Vol. 63, No. 4, 1881–1886, 2015.
22. Pandey, G. K., H. S. Singh, P. K. Bharti, and M. K. Meshram, "Metamaterial-based UWB antenna," *Electronics Letters*, Vol. 50, No. 18, 1266–1268, 2014.
23. Zhang, H. T., G. Q. Luo, B. Yuan, and X. H. Zhang, "A novel ultra-wideband metamaterial antenna using chessboard-shaped patch," *Microwave and Optical Technology Letters*, Vol. 58, No. 12, 3008–3012, 2016.
24. Liu, Z. G. and Y. X. Guo, "Compact low-profile dual band metamaterial antenna for body centric communications," *IEEE Antennas and Wireless Propagation Letters*, Vol. 14, 863–866, 2015.
25. Taghadosi, M., L. Albasha, N. Qaddoumi, and M. Ali, "Miniaturised printed elliptical nested fractal multiband antenna for energy harvesting applications," *IET Microwaves, Antennas & Propagation*, Vol. 9, No. 10, 1045–1053, 2015.
26. Du, G.-H., X. Tang, and F. Xiao, "Tri-band metamaterial-inspired monopole antenna with modified S-shaped resonator," *Progress In Electromagnetics Research Letters*, Vol. 23, 39–48, 2011.

27. Wang, Y. D., J. H. Lu, and H. M. Hsiao, "Novel design of semi-circular slot antenna with triple-band operation for WLAN/WIMAX communication," *Microwave and Optical Technology Letters*, Vol. 50, No. 6, 1531–1534, 2008.
28. Amani, N., M. Kamyab, A. Jafargholi, A. Hosseinbeig, and J. S. Meiguni, "Compact tri-band metamaterial-inspired antenna based on CRLH resonant structures," *Electronics Letters*, Vol. 50, No. 12, 847–848, 2014.
29. Azaro, R., E. Zeni, P. Rocca, and A. Massa, "Innovative design of a planar fractal-shaped GPS/GSM/Wi-Fi antenna," *Microwave and Optical Technology Letters*, Vol. 50, No. 3, 825–829, 2008.
30. Ali, T. and R. C. Biradar, "A compact multiband antenna using $\lambda/4$ rectangular stub loaded with metamaterial for IEEE 802.11 N and IEEE 802.16 E," *Microwave and Optical Technology Letters*, Vol. 59, No. 5, 1000–1006, 2017.
31. Zhao, Q., S.-X. Gong, W. Jiang, B. Yang, and J. Xie, "Compact wide-slot tri-band antenna for WLAN/WiMAX applications," *Progress In Electromagnetics Research Letters*, Vol. 18, 9–18, 2010.
32. Wang, Y. F., B. H. Sun, K. He, R. H. Li, and Y. J. Wang, "A compact tri-band antenna for WLAN/WiMAX applications," *Microwave and Optical Technology Letters*, Vol. 53, No. 10, 2371–2375, 2011.
33. Mathew, S., R. Anitha, U. Deepak, C. K. Aanandan, P. Mohanan, and K. Vasudevan, "A compact tri-band dual-polarized corner-truncated sectoral patch antenna," *IEEE Transactions on Antennas and Propagation*, Vol. 63, No. 12, 5842–5845, 2015.
34. Hu, W., J. J. Wu, S. F. Zheng, and J. Ren, "Compact ACS-fed printed antenna using dual edge resonators for tri-band operation," *IEEE Antennas and Wireless Propagation Letters*, Vol. 15, 207–210, 2016.
35. Pei, J., A. G. Wang, S. Gao, and W. Leng, "Miniaturized triple-band antenna with a defected ground plane for WLAN/WiMAX applications," *IEEE Antennas and Wireless Propagation Letters*, Vol. 10, 298–301, 2011.